Chinese Journal of Aeronautics 24 (2011) 484-492

Contents lists available at ScienceDirect

Chinese Journal of Aeronautics

journal homepage: www.elsevier.com/locate/cja

A Precise and Robust Control Strategy for Rigid Spacecraft Eigenaxis Rotation

CONG Binglong, LIU Xiangdong*, CHEN Zhen

School of Automation, Beijing Institute of Technology, Beijing 100081, China

Received 9 September 2010; revised 22 October 2010; accepted 25 April 2011

Abstract

Eigenaxis rotation is generally regarded as a near-minimum time strategy for rapid attitude maneuver due to its constitution of the shortest angular path between two orientations. In this paper, the robust control problem of rigid spacecraft eigenaxis rotation is investigated via time-varying sliding mode control (TVSMC) technique. Both external disturbance and parameter variation are taken into account. Major features of this robust eigenaxis rotation strategy are first demonstrated by a TVSMC algorithm. Global sliding phase is proved as well as the closed-loop system stability. Additionally, the necessary condition for eigenaxis rotation is provided. Subsequently, to suppress the global chattering and improve the control accuracy, a disturbance observer-based time-varying sliding mode control (DOTVSMC) algorithm is presented, where the boundary layer approach is used to soften the chattering and a disturbance observer is designed to attenuate undesired effect. The spacecraft attitude is represented by modified Rodrigues parameter (MRP) for the non-redundancy. Finally, a numerical simulation is employed to illustrate the effectiveness of the proposed strategy, where the pulse-width pulse-frequency (PWPF) technique is utilized to modulate the on-off thrusters.

Keywords: attitude control; eigenaxis maneuver; time-varying sliding mode control; global robust; disturbance observer; pulse-width pulse-frequency modulator

1. Introduction

Various strategies have been adopted in the past decades to implement spacecraft attitude maneuvers. Three major strategies, i.e., single-axis, multi-axis, and optimal, have been reported in the literature [1]. Particularly, single-axis strategy rotates each axis successively in some given order, which is easy to accomplish but at the expense of inefficiency with respect to time and fuel consumptions. Multi-axis strategy rotates two or three axes simultaneously, which tends to be fairly easy to implement and time-saving. Optimal strategy is proposed to minimize the propellant cost or maneuver time. However, most optimal algorithms require some specific mass properties such as axial symmetry. Based on past experience, multi-axis strategy provides an effective solution for spacecraft attitude maneuver due to its straightforward implementation, mass property independence, and generally good performance.

As a special case of three-axis strategy, eigenaxis rotation is generally regarded as a near-minimum time strategy for rapid attitude maneuver due to its constitution of the shortest angular path between two orientations. In the past decades, much research on eigenaxis rotation has been undertaken. In 1960s, the experience with Apollo has already shown the advantages of eigenaxis rotation [2]. Wie, et al. [3] presented an eigenaxis regulator with quaternion feedback. The proposed eigenaxis algorithm involved the linear feedback

*Corresponding author. Tel.: +86-10-68912460.
E-mail address: xdliu@bit.edu.cn
Foundation items: National Natural Science Foundation of China (108072030); Technology Innovation Program of Beijing Institute of Technology (CX0428)

doi: 10.1016/S1000-9361(11)60056-3

terms of quaternion and angular velocity together with the feed-forward of the gyroscopic coupling term, which has been successfully used for Apollo, Skylab, and Shuttle missions. Such an integration of feedback control and feed-forward control was further studied in Refs. [4]-[5]. To maneuver the spacecraft as fast as possible within the physical limits of actuators and sensors, Wie, et al. [4] further presented a feedback logic for eigenaxis rotation using cascade-saturation technique. Seywald, et al. [5] extended the eigenaxis regulator in Ref. [3] to the reorientation maneuvers, and several important properties such as the necessary condition for eigenaxis rotation were provided [5]. In addition, different actuators have been utilized to realize those eigenaxis algorithms such as the reaction wheels in Ref. [6] and the on-off thrusters in Ref. [7].

Recently, eigenaxis rotation has been revived as an attitude synchronization strategy in the formation flying [8-9]. In such an application, to achieve the attitude alignment among the formation, spacecraft should be rotated around the eigenaxis as accurately as possible. However, the eigenaxis algorithms mentioned above were designed for the ideal condition, i.e., neither parameter variation nor external disturbance was taken into account. The price paid for the robustness is that spacecraft is usually rotated deviating from the eigenaxis. Some effort has been made to derive robust eigenaxis algorithms. Cristi, et al. [10] approximated the eigenaxis algorithm in Ref. [3] by the adaptive approach. Both direct and indirect adaptive laws were designed when the inertia matrix is unknown. Moreover, Lawton, et al. [11] developed a model independent eigenaxis algorithm. Attitude maneuver was decomposed into two orthogonal successive rotations in Ref. [11], where the attitude motion perpendicular to the eigenaxis was damped by a high gain feedback. On the other hand, as a robust nonlinear control method, sliding mode control (SMC) has been widely used in attitude control system. However, it was generally believed that SMC could *not* execute the eigenaxis rotation in most cases due to the undesired dynamics in the reaching phase. It has been declared in Ref. [12] that an eigenaxis algorithm was presented via SMC. However, that proposition was based on the assumption that the gyroscopic torque, disturbance torque, and the torque needed for sliding-phase control can be neglected, which is hard to satisfy. Recently, a robust eigenaxis algorithm using time-varying sliding mode control (TVSMC) technique was proposed in Ref. [13], where the motion constraint imposed by eigenaxis rotation was satisfied by the dynamic behavior of the reduced system.

Even though much research has been undertaken over decades to address the robust control problem of eigenaxis rotations, there is still much work to be done. First, current investigations mainly focus on the rest-to-rest attitude maneuver. The more general case, i.e., the reorientation maneuver, requires deep-going research. Second, the *global* chattering problem has not received its due attention in the literature. In fact, due to the global sliding phase feature of the TVSMC technique, the chattering phenomenon exists throughout the entire control action, which is unacceptable in practice. Finally, the spacecraft control torque is provided by the on-off thrusters. The existing eigenaxis rotation algorithms generally assume that the actuators can produce the control torque command ideally. When the actuator dynamics is taken into account, the effectiveness of control algorithms needs to be verified. In this paper, we try to solve those problems in the TVSMC framework and present a precise and robust control strategy for rigid spacecraft eigenaxis rotations.

2. Mathematical Model and Problem Statement

2.1. Mathematical model

The attitude motion of the rigid spacecraft is characterized by the following equations [14]:

$$\boldsymbol{J}_{\mathrm{b}}\dot{\boldsymbol{\omega}}_{\mathrm{b}}+\boldsymbol{\omega}_{\mathrm{b}}^{\times}\boldsymbol{J}_{\mathrm{b}}\boldsymbol{\omega}_{\mathrm{b}}=\boldsymbol{T}_{\mathrm{b}}+\boldsymbol{T}_{\mathrm{d}} \tag{1}$$

$$\dot{\boldsymbol{\sigma}}_{\mathrm{b}}=\boldsymbol{M}(\boldsymbol{\sigma}_{\mathrm{b}})\boldsymbol{\omega}_{\mathrm{b}} \tag{2}$$

where all the quantities are expressed in the body fixed frame $\mathcal{F}_{\mathrm{B}}$, $\boldsymbol{J}_{\mathrm{b}}\in\mathbf{R}^{3\times3}$ is the spacecraft inertia matrix, $\boldsymbol{\omega}_{\mathrm{b}}=[\omega_1\quad\omega_2\quad\omega_3]^{\mathrm{T}}$ the angular velocity of spacecraft with respect to the inertial reference frame $\mathcal{F}_{\mathrm{I}}$, $\boldsymbol{T}_{\mathrm{b}}=[T_1\quad T_2\quad T_3]^{\mathrm{T}}$ the control torque offered by the on-off thrusters, and $\boldsymbol{T}_{\mathrm{d}}=[T_{\mathrm{d}1}\quad T_{\mathrm{d}2}\quad T_{\mathrm{d}3}]^{\mathrm{T}}$ the external disturbance torque. The superscript $(\cdot)^{\times}$ stands for the linear skew symmetric matrix operator for vector. For $\boldsymbol{\alpha}=[\alpha_1\quad\alpha_2\quad\alpha_3]^{\mathrm{T}}$, it is defined as follows:

$$\boldsymbol{\alpha}^{\times}=\begin{bmatrix}0&-\alpha_3&\alpha_2\\ \alpha_3&0&-\alpha_1\\ -\alpha_2&\alpha_1&0\end{bmatrix}$$

$\boldsymbol{\sigma}_{\mathrm{b}}=[\sigma_1\quad\sigma_2\quad\sigma_3]^{\mathrm{T}}$ is the modified Rodrigues parameter (MRP) representation of the inertial attitude, and $\boldsymbol{M}(\boldsymbol{\sigma}_{\mathrm{b}})$ is given by

$$\boldsymbol{M}(\boldsymbol{\sigma}_{\mathrm{b}})=\frac{(1-\|\boldsymbol{\sigma}_{\mathrm{b}}\|^2)\boldsymbol{I}_{3\times3}+2\boldsymbol{\sigma}_{\mathrm{b}}^{\times}+2\boldsymbol{\sigma}_{\mathrm{b}}\boldsymbol{\sigma}_{\mathrm{b}}^{\mathrm{T}}}{4}$$

with $\boldsymbol{I}_{3\times3}$ the 3×3 identity matrix and $\|\cdot\|$ the Euclid norm. Moreover, $\boldsymbol{M}^{\mathrm{T}}(\boldsymbol{\sigma}_{\mathrm{b}})\boldsymbol{M}(\boldsymbol{\sigma}_{\mathrm{b}})=m(\boldsymbol{\sigma}_{\mathrm{b}})\boldsymbol{I}_{3\times3}$, and $m(\boldsymbol{\sigma}_{\mathrm{b}})=(1+\|\boldsymbol{\sigma}_{\mathrm{b}}\|^2)^2/16$.

The transition matrix from $\mathcal{F}_{\mathrm{I}}$ to $\mathcal{F}_{\mathrm{B}}$ in terms of MRP is given by

$$\boldsymbol{R}(\boldsymbol{\sigma}_{\mathrm{b}})=\boldsymbol{R}_{\mathrm{BI}}=\boldsymbol{I}_{3\times3}+\frac{8\boldsymbol{\sigma}_{\mathrm{b}}^{\times}\boldsymbol{\sigma}_{\mathrm{b}}^{\times}-4(1-\|\boldsymbol{\sigma}_{\mathrm{b}}\|^2)\boldsymbol{\sigma}_{\mathrm{b}}^{\times}}{(1+\|\boldsymbol{\sigma}_{\mathrm{b}}\|^2)^2}$$

In this paper, we will focus on the set point control problem of reorienting a spacecraft from an arbitrary attitude to a steady desired attitude $\boldsymbol{\sigma}_{\mathrm{d}}$. Define the error MRP as

$$\boldsymbol{\sigma}_{\mathrm{e}}=\boldsymbol{\sigma}_{\mathrm{d}}\oplus\boldsymbol{\sigma}_{\mathrm{b}}^{*}=[\sigma_{\mathrm{e}1}\quad\sigma_{\mathrm{e}2}\quad\sigma_{\mathrm{e}3}]^{\mathrm{T}} \tag{3}$$

where $\boldsymbol{\sigma}_{\mathrm{b}}^{*}$ is the inverse of $\boldsymbol{\sigma}_{\mathrm{b}}$, which is extracted from the inverse of $\boldsymbol{R}(\boldsymbol{\sigma}_{\mathrm{b}})$ and $\boldsymbol{\sigma}_{\mathrm{b}}^{*}=-\boldsymbol{\sigma}_{\mathrm{b}}$, and "⊕" is the MRP multiplication operator. For two MRPs, e.g., $\boldsymbol{\sigma}_x$ and $\boldsymbol{\sigma}_y$, it is defined as [15]

$$\boldsymbol{\sigma}_x \oplus \boldsymbol{\sigma}_y = \frac{(1-\|\boldsymbol{\sigma}_y\|^2)\boldsymbol{\sigma}_x + (1-\|\boldsymbol{\sigma}_x\|^2)\boldsymbol{\sigma}_y - 2\boldsymbol{\sigma}_x^{\times}\boldsymbol{\sigma}_y}{1+\|\boldsymbol{\sigma}_y\|^2\|\boldsymbol{\sigma}_x\|^2 - 2\boldsymbol{\sigma}_y^{\mathrm{T}}\boldsymbol{\sigma}_x} \tag{4}$$

Correspondingly, the error kinematics is described as

$$\dot{\boldsymbol{\sigma}}_{\mathrm{e}} = -\boldsymbol{M}^{\mathrm{T}}(\boldsymbol{\sigma}_{\mathrm{e}})\boldsymbol{\omega}_{\mathrm{b}} \tag{5}$$

Furthermore, the inertia matrix uncertainty is taken into account. Let $\boldsymbol{J}_{\mathrm{b}}=\hat{\boldsymbol{J}}_{\mathrm{b}}+\delta\boldsymbol{J}_{\mathrm{b}}$ with $\delta\boldsymbol{J}_{\mathrm{b}}$ the uncertainty caused by the change in mass properties and $\hat{\boldsymbol{J}}_{\mathrm{b}}=\mathrm{diag}(J_1, J_2, J_3)$ the nominal inertia matrix. Then the attitude dynamics is described as

$$\hat{\boldsymbol{J}}_{\mathrm{b}}\dot{\boldsymbol{\omega}}_{\mathrm{b}} + \boldsymbol{\omega}_{\mathrm{b}}^{\times}\hat{\boldsymbol{J}}_{\mathrm{b}}\boldsymbol{\omega}_{\mathrm{b}} = \boldsymbol{T}_{\mathrm{b}} - \delta\boldsymbol{J}_{\mathrm{b}}\dot{\boldsymbol{\omega}}_{\mathrm{b}} - \boldsymbol{\omega}_{\mathrm{b}}^{\times}\delta\boldsymbol{J}_{\mathrm{b}}\boldsymbol{\omega}_{\mathrm{b}} + \boldsymbol{T}_{\mathrm{d}} \tag{6}$$

According to the structural feature in Eq. (6), we can lump all the elements caused by inertia matrix uncertainty and external disturbance as the lumped disturbance, i.e., $\boldsymbol{\Delta}_{\mathrm{du}}=-\delta\boldsymbol{J}_{\mathrm{b}}\dot{\boldsymbol{\omega}}_{\mathrm{b}} - \boldsymbol{\omega}_{\mathrm{b}}^{\times}\delta\boldsymbol{J}_{\mathrm{b}}\boldsymbol{\omega}_{\mathrm{b}}+\boldsymbol{T}_{\mathrm{d}}$. Then, the attitude dynamics is rewritten as

$$\hat{\boldsymbol{J}}_{\mathrm{b}}\dot{\boldsymbol{\omega}}_{\mathrm{b}} + \boldsymbol{\omega}_{\mathrm{b}}^{\times}\hat{\boldsymbol{J}}_{\mathrm{b}}\boldsymbol{\omega}_{\mathrm{b}} = \boldsymbol{T}_{\mathrm{b}} + \boldsymbol{\Delta}_{\mathrm{du}} \tag{7}$$

It is clear that the lumped disturbance is matched to the system. Furthermore, it is assumed that the lumped disturbance is not exactly known, but an upper bound is available, i.e., $\|\boldsymbol{\Delta}_{\mathrm{du}}\|_{\infty}\le d_{\max}$ with $\|\cdot\|_{\infty}$ being the infinite norm.

2.2. Problem statement

On the basis of Euler principal rotation theorem, the time evolution of error MRP in terms of principal elements can be expressed as

$$\boldsymbol{\sigma}_{\mathrm{e}}(t) = \tan\frac{\phi(t)}{4}\boldsymbol{n} \tag{8}$$

where $\boldsymbol{n}=[n_1 \quad n_2 \quad n_3]^{\mathrm{T}}$ is the unit eigenaxis vector and $\phi(t)$ the principal angle. $\boldsymbol{n}$ is a judicious axis fixed in both initial and final orientations [15]. From Eq. (8), it is easy to obtain $\boldsymbol{n}=\boldsymbol{\sigma}_{\mathrm{e}}(0)/\|\boldsymbol{\sigma}_{\mathrm{e}}(0)\|$. Then the motion constraint imposed by the eigenaxis rotation can be characterized by [16]:

$$\boldsymbol{\omega}_{\mathrm{b}}(t)\times\boldsymbol{n} = \boldsymbol{0} \tag{9}$$

The control objective is not only to accomplish the desired reorientation maneuver but also to implement the maneuver as an eigenaxis rotation in the presence of disturbance and parameter variation. This problem can be summarized as follows:

Find a controller such that

$$\begin{cases} \lim\limits_{t\to\infty}\boldsymbol{\sigma}_{\mathrm{e}}(t) = \lim\limits_{t\to\infty}\boldsymbol{\omega}_{\mathrm{b}}(t) = \boldsymbol{0} \\ \boldsymbol{\omega}_{\mathrm{b}}(t)\times\boldsymbol{n} = \boldsymbol{0} \end{cases}$$

3. Main Results

3.1. Robust eigenaxis algorithm via TVSMC

In this section, an eigenaxis algorithm via TVSMC method is designed to guarantee the eigenaxis rotation performance in the presence of inertia matrix uncertainty and external disturbance.

First, a time-varying sliding surface is defined as

$$\boldsymbol{S}(t) = \boldsymbol{\omega}_{\mathrm{b}} - \lambda\frac{\boldsymbol{M}(\boldsymbol{\sigma}_{\mathrm{e}})}{m(\boldsymbol{\sigma}_{\mathrm{e}})}(\boldsymbol{\sigma}_{\mathrm{e}} + \boldsymbol{\zeta}\mathrm{e}^{-\lambda t}) = \boldsymbol{0} \tag{10}$$

where $\boldsymbol{S}(t) = [s_1(t) \quad s_2(t) \quad s_3(t)]^{\mathrm{T}}$ is the time-varying sliding function, $\lambda\in\mathbf{R}^{+}$, and $\boldsymbol{\zeta} = [\zeta_1 \quad \zeta_2 \quad \zeta_3]^{\mathrm{T}}$ is the coefficient vector related to the initial system states. In the following derivations, we will denote $\boldsymbol{M}(\boldsymbol{\sigma}_{\mathrm{e}})$ and $m(\boldsymbol{\sigma}_{\mathrm{e}})$ by $\boldsymbol{M}$ and m for clarity.

According to the basic idea of TVSMC technique, the time-varying sliding surface passes through the initial system states at the start of the motion and then moves towards a predetermined time-invariant sliding surface [17]. Therefore, we can determine $\boldsymbol{\zeta}$ by letting $\boldsymbol{S}(0)=\boldsymbol{0}$, then

$$\boldsymbol{\zeta} = \frac{\boldsymbol{M}^{\mathrm{T}}\boldsymbol{\omega}_{\mathrm{b}}(0) - \lambda\boldsymbol{\sigma}_{\mathrm{e}}(0)}{\lambda} \tag{11}$$

Consider the following Lyapunov function:

$$V = \frac{1}{2}\boldsymbol{S}^{\mathrm{T}}(t)\hat{\boldsymbol{J}}\boldsymbol{S}(t) \tag{12}$$

The TVSMC algorithm is designed to produce a negative definite derivative of the above Lyapunov function, which is described by

$$\begin{aligned} \boldsymbol{T}_{\mathrm{b}} &= \boldsymbol{u}_{\mathrm{eq}} + \boldsymbol{u}_{\mathrm{sw}} = \\ &\boldsymbol{\omega}_{\mathrm{b}}^{\times}\hat{\boldsymbol{J}}_{\mathrm{b}}\boldsymbol{\omega}_{\mathrm{b}} - \frac{2\lambda\hat{\boldsymbol{J}}_{\mathrm{b}}(2\boldsymbol{M}^{\mathrm{T}} - \boldsymbol{\sigma}_{\mathrm{e}}\boldsymbol{\sigma}_{\mathrm{e}}^{\mathrm{T}})\boldsymbol{\omega}_{\mathrm{b}}}{1+\|\boldsymbol{\sigma}_{\mathrm{e}}\|^2} + \\ &\lambda\hat{\boldsymbol{J}}_{\mathrm{b}}\left[\frac{\mathrm{d}}{\mathrm{d}t}\left(\frac{\boldsymbol{M}\boldsymbol{\zeta}}{m}\right) - \frac{\lambda\boldsymbol{M}\boldsymbol{\zeta}}{m}\right]\mathrm{e}^{-\lambda t} - \boldsymbol{\Gamma}\,\mathrm{sgn}\,\boldsymbol{S}(t) \end{aligned} \tag{13}$$

where $\boldsymbol{u}_{\mathrm{eq}}$ is the equivalent control component derived from $\dot{\boldsymbol{S}}(t)=\boldsymbol{0}$ in the absence of the lumped disturbance, $\boldsymbol{u}_{\mathrm{sw}}=-\boldsymbol{\Gamma}\,\mathrm{sgn}\,\boldsymbol{S}(t)$ the discontinuous switching control component, $\boldsymbol{\Gamma}=\mathrm{diag}(\gamma_1, \gamma_2, \gamma_3)$ the switching gain matrix with its element $\gamma_i > d_{\max}$ (i=1, 2, 3), $\mathrm{sgn}\,\boldsymbol{S}(t)=[\mathrm{sgn}\,s_1(t) \quad \mathrm{sgn}\,s_2(t) \quad \mathrm{sgn}\,s_3(t)]^{\mathrm{T}}$, and $\mathrm{d}(\boldsymbol{M}\boldsymbol{\zeta}/m)/\mathrm{d}t$ the time derivative of $\boldsymbol{M}\boldsymbol{\zeta}/m$. Especially, if we let $\boldsymbol{\beta} = [\sigma_{\mathrm{e}3}\zeta_2 \quad \sigma_{\mathrm{e}1}\zeta_3 \quad \sigma_{\mathrm{e}2}\zeta_1]^{\mathrm{T}}$ and $\boldsymbol{\upsilon} = [\sigma_{\mathrm{e}2}\zeta_3 \quad \sigma_{\mathrm{e}3}\zeta_1 \quad \sigma_{\mathrm{e}1}\zeta_2]^{\mathrm{T}}$, then we can get

$$\frac{\mathrm{d}}{\mathrm{d}t}\left(\frac{\boldsymbol{M}\boldsymbol{\zeta}}{m}\right) = \frac{8[\boldsymbol{\sigma}_{\mathrm{e}}^{\mathrm{T}}\boldsymbol{\zeta}\boldsymbol{I}_{3\times3} - (\boldsymbol{\zeta}-\boldsymbol{\beta}+\boldsymbol{\upsilon})^{\times}]}{(1+\|\boldsymbol{\sigma}_{\mathrm{e}}\|^2)^2} - \frac{4\boldsymbol{M}\boldsymbol{\zeta}\boldsymbol{\sigma}_{\mathrm{e}}^{\mathrm{T}}}{(1+\|\boldsymbol{\sigma}_{\mathrm{e}}\|)m}$$

Before moving on, a lemma is firstly introduced.

Lemma 1 A *global sliding phase* would be achieved if the system in Eq. (5) and Eq. (7) is controlled by the TVSMC algorithm in Eq. (13), i.e., for

$\forall t\in[0,\infty)$, $\boldsymbol{S}(t)\equiv\boldsymbol{0}$.

Proof See the Appendix A.

As shown in Lemma 1, the proposed TVSMC algorithm eliminates the reaching phase in the SMC and a global sliding motion is achieved. According to the variable structure control theory, this feature implies that the system is *global robust* against matched model uncertainty and external disturbance.

Based on Lemma 1, the following theorem is obtained:

Theorem 1 For the system in Eq. (5) and Eq. (7), by adopting the TVSMC algorithm in Eq. (13), then

(1) The closed system is *almost* global asymptotically stable;

(2) The attitude maneuver would be performed as an eigenaxis rotation, if the initial angular velocity is collinear with the initial error MRP.

Proof As shown in Lemma 1, the time-varying sliding function equals to zero for $\forall t\in[0,\infty)$, then from Eq. (10), we can conclude

$$\boldsymbol{\omega}_{\mathrm{b}}=\lambda\frac{\boldsymbol{M}(\boldsymbol{\sigma}_{\mathrm{e}}+\boldsymbol{\zeta}\mathrm{e}^{-\lambda t})}{m} \tag{14}$$

By substituting Eq. (14) into Eq. (5), we can get the following first-order three-dimensional vector differential equation:

$$\dot{\boldsymbol{\sigma}}_{\mathrm{e}}+\lambda\boldsymbol{\sigma}_{\mathrm{e}}+\lambda\mathrm{e}^{-\lambda t}\boldsymbol{\zeta}=\boldsymbol{0} \tag{15}$$

The analytical result is obtained for $\boldsymbol{\sigma}_{\mathrm{e}}(t)$ as

$$\boldsymbol{\sigma}_{\mathrm{e}}(t)=\mathrm{e}^{-\lambda t}(\boldsymbol{\sigma}_{\mathrm{e}}(0)-\lambda t\boldsymbol{\zeta}) \tag{16}$$

As mentioned before, $\boldsymbol{\zeta}$ is a constant vector. Then, from Eq. (16) and the relationship in Eq. (14), it is obvious that $\lim\limits_{t\to\infty}\boldsymbol{\sigma}_{\mathrm{e}}(t)=\lim\limits_{t\to\infty}\boldsymbol{\omega}_{\mathrm{b}}(t)=\boldsymbol{0}$. However, as shown in Theorem 1 of Ref. [18], no point of SO(3)×$\mathbf{R}^3$ can be a globally asymptotically stable equilibrium of Eq. (5) and Eq. (7), which hence causes unwinding in the attitude responses. Therefore, the term of *almost* global asymptotic stability is used.

Furthermore, if the initial angular velocity and the initial error MRP are collinear, we can define

$$\boldsymbol{\omega}_{\mathrm{b}}(0)=k\boldsymbol{\sigma}_{\mathrm{e}}(0) \tag{17}$$

where k is a proper scalar.

Then Eq. (11) can be described as

$$\boldsymbol{\zeta}=\frac{k\boldsymbol{M}^{\mathrm{T}}\boldsymbol{\sigma}_{\mathrm{e}}(0)-\lambda\boldsymbol{\sigma}_{\mathrm{e}}(0)}{\lambda}=\frac{k(1+\|\boldsymbol{\sigma}_{\mathrm{e}}(0)\|^2)-4\lambda}{4\lambda}\boldsymbol{\sigma}_{\mathrm{e}}(0) \tag{18}$$

Furthermore, we can get the following analytical expression for $\boldsymbol{\sigma}_{\mathrm{e}}(t)$ and $\boldsymbol{\omega}_{\mathrm{b}}(t)$:

$$\boldsymbol{\sigma}_{\mathrm{e}}(t)=p(t)\boldsymbol{\sigma}_{\mathrm{e}}(0) \tag{19}$$

$$\boldsymbol{\omega}_{\mathrm{b}}(t)=q(t)\boldsymbol{\sigma}_{\mathrm{e}}(0) \tag{20}$$

where $p(t)$ and $q(t)$ are scalar functions, which are given by

$$p(t)=\frac{4-[k(1+\|\boldsymbol{\sigma}_{\mathrm{e}}(0)\|^2)-4\lambda]t}{4}\mathrm{e}^{-\lambda t}$$

$$q(t)=\frac{4\lambda p(t)+\mathrm{e}^{-\lambda t}[k(1+\|\boldsymbol{\sigma}_{\mathrm{e}}(0)\|^2)-4\lambda]}{1+p^2(t)\|\boldsymbol{\sigma}_{\mathrm{e}}(0)\|^2}$$

As $\boldsymbol{n}=\boldsymbol{\sigma}_{\mathrm{e}}(0)/\|\boldsymbol{\sigma}_{\mathrm{e}}(0)\|$, the conclusion that $\boldsymbol{\omega}_{\mathrm{b}}\times\boldsymbol{n}=\boldsymbol{0}$ can be drawn.

Especially, for a special case of rest-to-rest attitude maneuver, the above results can be further enhanced. In this case, we have $k=0$. Then the scalar functions in Eqs. (19)-(20) can be rewritten as

$$p(t)=\mathrm{e}^{-\lambda t}(1+\lambda t) \tag{21}$$

$$q(t)=\frac{4\lambda^2\mathrm{e}^{-\lambda t}t}{1+p^2(t)\|\boldsymbol{\sigma}_{\mathrm{e}}(0)\|^2} \tag{22}$$

By a simple extreme judgment of Eq. (21), we can conclude that $p(t)$ is monotonically decreasing and there is no overshooting of the error MRP response. And, more importantly, if the slew rate is constrained by physical limit such as the sensor saturation, Eq. (22) provides an effective way for the control parameter tuning.

3.2. A precise and robust eigenaxis algorithm via disturbance observer-based time-varying sliding mode control (DOTVSMC)

As outlined in Section 3.1, the global sliding phase of TVSMC guarantees the global robustness against matched parameter variation and external disturbance. However, such a feature also implies that the undesired chattering phenomenon exists throughout the motion, which has not been extensively investigated in current TVSMC studies.

It is well known that smooth functions are generally used to replace the sign function in the control algorithm in order to deal with the chattering problem in SMC, which include saturation function, hysteresis, and hysteresis with saturation. Then, the switching control is modified as $\boldsymbol{u}_{\mathrm{sw}}=-\boldsymbol{\Gamma}\boldsymbol{\xi}^{-1}\mathrm{sat}\,\boldsymbol{S}(t)$ with the saturation function defined by

$$\mathrm{sat}\,s_i(t)=\begin{cases}\dfrac{s_i(t)}{\xi_i} & |s_i(t)|\le\xi_i\\ \mathrm{sgn}\,s_i(t) & |s_i(t)|>\xi_i\end{cases}$$

where i=1, 2, 3, $\boldsymbol{\xi}=\mathrm{diag}(\xi_1,\ \xi_2,\ \xi_3)$, and ξ_i is the boundary layer thickness which will soften or eliminate the chattering if appropriately chosen. However, there is a trade-off in the selection of ξ_i. The thicker the boundary layer is, the better the chattering will be suppressed. However, the static error inside the boundary layer will be larger, and vice versa. When this chattering reduction method is applied to TVSMC

algorithm, the problem of detriment of robustness and precision still exists. Therefore, the robust eigenaxis algorithm in Eq. (13) with the boundary layer is enhanced by a disturbance observer (DOB) in this section, which would reduce the static error inside the boundary layer while suppress the global chattering.

First, a semi-deterministic waveform model is utilized to model the lumped disturbance in Eq. (7) [19]:

$$\boldsymbol{\Delta}_{\mathrm{du}}=\begin{bmatrix} w_{11}f_{11}(t)+w_{12}f_{12}(t)+\cdots+w_{1n}f_{1n}(t) \\ w_{21}f_{21}(t)+w_{22}f_{22}(t)+\cdots+w_{2n}f_{2n}(t) \\ w_{31}f_{31}(t)+w_{32}f_{32}(t)+\cdots+w_{3n}f_{3n}(t) \end{bmatrix} \tag{23}$$

where w_{ij} (i=1, 2, 3; j=1, 2, ⋯, n) is the weight coefficient and $f_{ij}(t)$ the basis function. It is further assumed that the basis function $f_{ij}(t)$ satisfies a linear differential equation, which means that the lumped disturbance is generated by a linear exogenous system. The state space expression of the lumped disturbance is described by [20]

$$\begin{cases} \dot{\boldsymbol{z}}=\boldsymbol{D}\boldsymbol{z} \\ \boldsymbol{\Delta}_{\mathrm{du}}=\boldsymbol{H}\boldsymbol{z} \end{cases} \tag{24}$$

where $\boldsymbol{z}=[z_{11}\ \cdots\ z_{1n}\ z_{21}\cdots\ z_{2n}\ z_{31}\cdots\ z_{3n}]^{\mathrm{T}}$ is the state variable with $z_{i1}=(\boldsymbol{\Delta}_{\mathrm{du}})_i$, $\dot{z}_{in}=0$, and $z_{i(j+1)}=\dot{z}_{ij}$; $\boldsymbol{H}\in\mathbf{R}^{3\times 3n}$ is the output matrix and $\boldsymbol{D}\in\mathbf{R}^{3n\times 3n}$ the system matrix.

Based on the characteristics of the space disturbance and the effect of the inertia matrix uncertainty, the semi-deterministic waveform model used in this paper is selected as

$$\boldsymbol{\Delta}_{\mathrm{du}}=\begin{bmatrix} w_{11}+w_{12}t+w_{13}t^2 \\ w_{21}+w_{22}t+w_{23}t^2 \\ w_{31}+w_{32}t+w_{33}t^2 \end{bmatrix} \tag{25}$$

As $\mathrm{d}^3\boldsymbol{\Delta}_{\mathrm{du}}/\mathrm{d}t^3=0$, then output matrix and system matrix in Eq. (24) are given by

$$\boldsymbol{H}=\begin{bmatrix} \boldsymbol{H}_1 & \mathbf{0}_{1\times 3} & \mathbf{0}_{1\times 3} \\ \mathbf{0}_{1\times 3} & \boldsymbol{H}_2 & \mathbf{0}_{1\times 3} \\ \mathbf{0}_{1\times 3} & \mathbf{0}_{1\times 3} & \boldsymbol{H}_3 \end{bmatrix}\in\mathbf{R}^{3\times 9} \tag{26}$$

$$\boldsymbol{D}=\begin{bmatrix} \boldsymbol{D}_1 & \mathbf{0}_{3\times 3} & \mathbf{0}_{3\times 3} \\ \mathbf{0}_{3\times 3} & \boldsymbol{D}_2 & \mathbf{0}_{3\times 3} \\ \mathbf{0}_{3\times 3} & \mathbf{0}_{3\times 3} & \boldsymbol{D}_3 \end{bmatrix}\in\mathbf{R}^{9\times 9} \tag{27}$$

with $\boldsymbol{H}_i=[1\quad 0\quad 0]$, $\boldsymbol{D}_i=\begin{bmatrix} 0 & 1 & 0 \\ 0 & 0 & 1 \\ 0 & 0 & 0 \end{bmatrix}$ (i=1, 2, 3). The subscript of $\mathbf{0}$ denotes the zero matrix with appropriate dimensions.

Here, we present the DOTVSMC algorithm as

$$\boldsymbol{T}_{\mathrm{b}}=\boldsymbol{u}_{\mathrm{eq}}+\boldsymbol{u}_{\mathrm{sw}}-\boldsymbol{u}_{\mathrm{ob}} \tag{28}$$

with the following DOB:

$$\begin{cases} \dot{\hat{\boldsymbol{z}}}=\boldsymbol{D}\hat{\boldsymbol{z}}-\boldsymbol{K}_0(\boldsymbol{z}-\hat{\boldsymbol{z}}) \\ \hat{\boldsymbol{\Delta}}_{\mathrm{du}}=\boldsymbol{H}\hat{\boldsymbol{z}} \end{cases} \tag{29}$$

where $\boldsymbol{u}_{\mathrm{ob}}=\hat{\boldsymbol{\Delta}}_{\mathrm{du}}$ is the observed value of the lumped disturbance and $\boldsymbol{K}_0\in\mathbf{R}^{9\times 9}$ the observer gain matrix. The initial value of $\hat{\boldsymbol{z}}$ is supposed to be $\mathbf{0}_{9\times 1}$.

However, the DOB in Eq. (29) cannot be directly implemented due to the immeasurable state $\boldsymbol{z}$ (or equivalently, the unavailable angular acceleration $\dot{\boldsymbol{\omega}}_{\mathrm{b}}$). Therefore, a $\boldsymbol{Q}$ filter is utilized. Define the auxiliary variable $\boldsymbol{Q}$ as

$$\boldsymbol{Q}=\hat{\boldsymbol{z}}-\boldsymbol{K}_1\boldsymbol{S}(t) \tag{30}$$

where $\boldsymbol{K}_1\in\mathbf{R}^{9\times 3}$ is the gain matrix and satisfies the following condition:

$$\boldsymbol{K}_0+\boldsymbol{K}_1\hat{\boldsymbol{J}}_{\mathrm{b}}^{-1}\boldsymbol{H}=\mathbf{0}_{9\times 9} \tag{31}$$

Then, the modified DOB composed by the measurable or known states is given by

$$\begin{aligned} \dot{\boldsymbol{Q}}=&(\boldsymbol{D}+\boldsymbol{K}_0)\boldsymbol{Q}+(\boldsymbol{D}+\boldsymbol{K}_0)\boldsymbol{K}_1\boldsymbol{S}(t)- \\ &\boldsymbol{K}_1\hat{\boldsymbol{J}}_{\mathrm{b}}^{-1}(\boldsymbol{u}_{\mathrm{sw}}+\boldsymbol{u}_{\mathrm{ob}}) \end{aligned} \tag{32}$$

and $\boldsymbol{Q}(0)=\hat{\boldsymbol{z}}(0)-\boldsymbol{K}_1\boldsymbol{S}(0)=\mathbf{0}_{9\times 1}$.

If we define the estimation error of $\boldsymbol{Q}$ as

$$\Delta\boldsymbol{Q}=(\hat{\boldsymbol{z}}-\boldsymbol{K}_1\boldsymbol{S}(t))-(\boldsymbol{z}-\boldsymbol{K}_1\boldsymbol{S}(t)) \tag{33}$$

By substituting Eq. (33) into Eq. (32), we can get the following estimation error dynamics:

$$\Delta\dot{\boldsymbol{Q}}=(\boldsymbol{D}+\boldsymbol{K}_0)\Delta\boldsymbol{Q} \tag{34}$$

From Eq. (34), we can see that if the gain matrix $\boldsymbol{K}_0$ is selected large enough then the estimation error dynamics is global asymptotically stable.

To sum up, the complete DOTVSMC algorithm is described by the following equations:

$$\begin{cases} \boldsymbol{T}_{\mathrm{b}}=\boldsymbol{u}_{\mathrm{eq}}+\boldsymbol{u}_{\mathrm{sw}}-\boldsymbol{u}_{\mathrm{ob}} \\ \boldsymbol{u}_{\mathrm{ob}}=\hat{\boldsymbol{\Delta}}_{\mathrm{du}} \\ \hat{\boldsymbol{\Delta}}_{\mathrm{du}}=\boldsymbol{H}\hat{\boldsymbol{z}} \\ \hat{\boldsymbol{z}}=\boldsymbol{Q}+\boldsymbol{K}_1\boldsymbol{S}(t) \\ \dot{\boldsymbol{Q}}=(\boldsymbol{D}+\boldsymbol{K}_0)\boldsymbol{Q}+(\boldsymbol{D}+\boldsymbol{K}_0)\boldsymbol{K}_1\boldsymbol{S}(t)- \\ \quad\boldsymbol{K}_1\hat{\boldsymbol{J}}_{\mathrm{b}}^{-1}(\boldsymbol{u}_{\mathrm{sw}}+\boldsymbol{u}_{\mathrm{ob}}) \end{cases} \tag{35}$$

Now, we will study the system behavior inside the boundary layer of both TVSMC and DOTVSMC to demonstrate the improvement of DOTVSMC in the control accuracy.

For the DOTVSMC algorithm, the time derivative of the time-varying sliding function is described as

$$\dot{\boldsymbol{S}}(t)=\hat{\boldsymbol{J}}_{\mathrm{b}}^{-1}(-\boldsymbol{\Gamma}\boldsymbol{\xi}^{-1}\boldsymbol{S}(t)+\boldsymbol{\Delta}_{\mathrm{du}}-\hat{\boldsymbol{\Delta}}_{\mathrm{du}}) \tag{36}$$

On the other hand, the time derivative of the time-

varying sliding function in TVSMC is expressed as

$$\dot{\boldsymbol{S}}(t)=\hat{\boldsymbol{J}}_{\mathrm{b}}^{-1}(-\boldsymbol{\Gamma}\boldsymbol{\xi}^{-1}\boldsymbol{S}(t)+\boldsymbol{\Delta}_{\mathrm{du}}) \tag{37}$$

Denote the static value of the time-varying sliding function inside the boundary layer of DOTVSMC and TVSMC as $\boldsymbol{S}_{\mathrm{d}}$ and $\boldsymbol{S}_{\mathrm{t}}$. Then, let $\dot{\boldsymbol{S}}(t)=\boldsymbol{0}$, we can get

$$\begin{cases}\boldsymbol{S}_{\mathrm{d}}=(\boldsymbol{\Gamma}\boldsymbol{\xi}^{-1})^{-1}(\boldsymbol{\Delta}_{\mathrm{du}}-\hat{\boldsymbol{\Delta}}_{\mathrm{du}})\\ \boldsymbol{S}_{\mathrm{t}}=(\boldsymbol{\Gamma}\boldsymbol{\xi}^{-1})^{-1}\boldsymbol{\Delta}_{\mathrm{du}}\end{cases} \tag{38}$$

From Eq. (38), it is obvious that the static value of $\boldsymbol{S}(t)$ by DOTVSMC is much smaller than that of TVSMC after the convergence of DOB. According to the definition of $\boldsymbol{S}(t)$ in Eq. (10), this feature implies that a more precise control performance is achieved by DOTVSMC.

4. Simulation Results and Discussion

In this section, a numerical simulation is employed to test the proposed eigenaxis rotation strategy. For simplicity, a rest-to-rest reorientation maneuver is considered in the simulation.

Suppose that the inertia matrix for the controller design is given by $\hat{\boldsymbol{J}}_{\mathrm{b}}=\mathrm{diag}(48,25,61.8)$ and the uncertainty is 10% of the nominal value. The external disturbance is $\boldsymbol{T}_{\mathrm{d}}=[1+0.2\sin(0.01t)\quad 1+0.2\sin(0.01t)\quad 2\cdot(1+0.2\sin(0.01t))]\times10^{-1}$ N·m. The initial attitude variables of the spacecraft are $\boldsymbol{\sigma}_{\mathrm{b}}(0)=[-0.2\quad 0.3\quad 0.1]^{\mathrm{T}}$ and $\boldsymbol{\omega}_{\mathrm{b}}(0)=\boldsymbol{0}$ rad/s. The desired steady attitude is $\boldsymbol{\sigma}_{\mathrm{d}}=[0.1\quad 0.2\quad -0.3]^{\mathrm{T}}$. The maneuver is equivalent to an eigenaxis rotation around $\boldsymbol{n}=[0.92\quad 0.02\quad -0.39]^{\mathrm{T}}$ about 106°.

The parameters for the DOTVSMC algorithm are λ=0.25, $\boldsymbol{\Gamma}=\mathrm{diag}(0.9, 0.9, 0.9)$, $\boldsymbol{\xi}=\boldsymbol{I}_{3\times3}\times10^{-3}$, and

$$\begin{cases}\boldsymbol{K}_0=\begin{bmatrix}\boldsymbol{K}_{01} & \boldsymbol{0}_{3\times3} & \boldsymbol{0}_{3\times3}\\ \boldsymbol{0}_{3\times3} & \boldsymbol{K}_{02} & \boldsymbol{0}_{3\times3}\\ \boldsymbol{0}_{3\times3} & \boldsymbol{0}_{3\times3} & \boldsymbol{K}_{03}\end{bmatrix}\\ \boldsymbol{K}_{0i}=\begin{bmatrix}-18 & 0 & 0\\ -180 & 0 & 0\\ -600 & 0 & 0\end{bmatrix}\qquad (i=1,2,3)\end{cases}$$

Based on the characteristic of eigenaxis rotation, we adopt the Euclid norm of the motion constraint in Eq. (9) to evaluate the eigenaxis rotation performance. It is clear that $\|\boldsymbol{\omega}_{\mathrm{b}}\times\boldsymbol{n}\|$ should be identically equal to zero if an ideal eigenaxis rotation is performed. Moreover, to test the effectiveness of DOB, we define the estimation error as $\boldsymbol{e}=\boldsymbol{\Delta}_{\mathrm{du}}-\hat{\boldsymbol{\Delta}}_{\mathrm{du}}$ with $\boldsymbol{e}=[e_1\quad e_2\quad e_3]^{\mathrm{T}}$.

To demonstrate the major features of the proposed eigenaxis algorithms, we firstly assume that the actuators can realize the control torque commands ideally just as Ref. [7] and Ref. [13]. The comparison results of TVSMC and DOTVSMC are shown in Figs. 1-6.

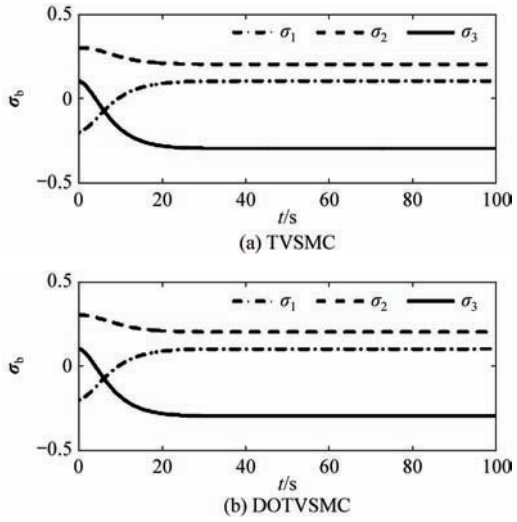

Fig. 1 Comparison of inertial MRP evolutions.

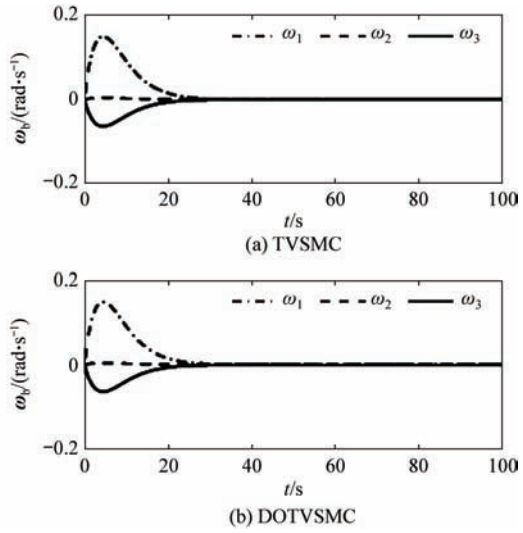

Fig. 2 Comparison of angular velocity responses.

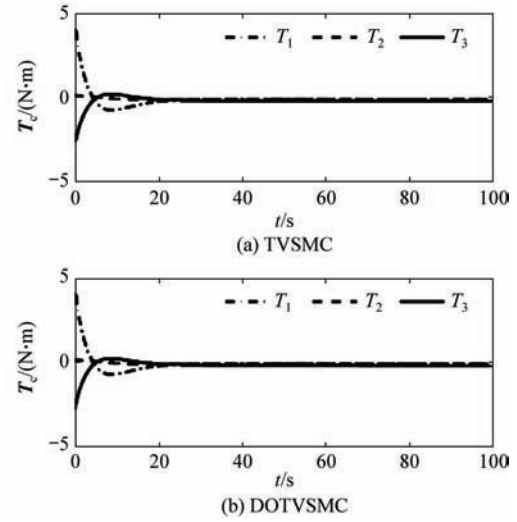

Fig. 3 Comparison of control torque commands.

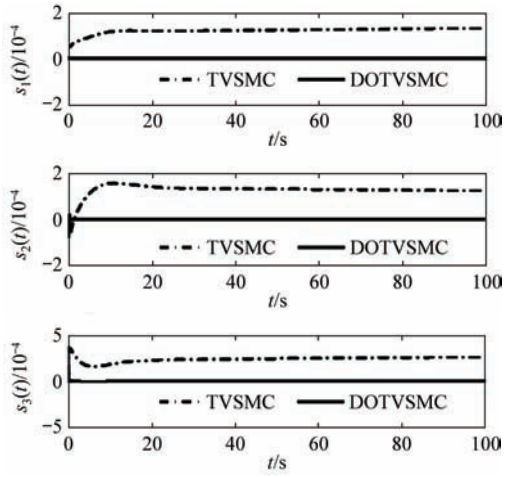

Fig. 4 Comparison of time-varying sliding functions with boundary layer approximation.

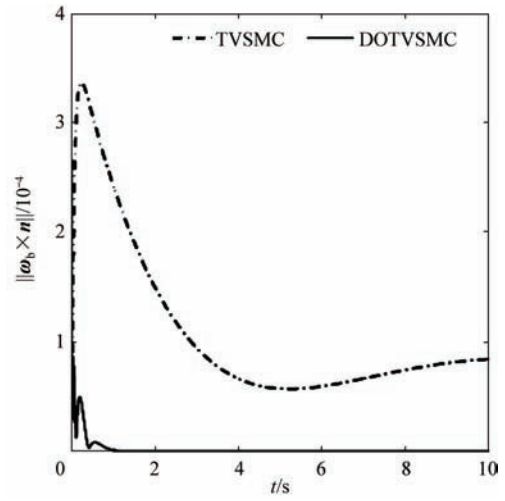

Fig. 5 Comparison of eigenaxis rotation performance.

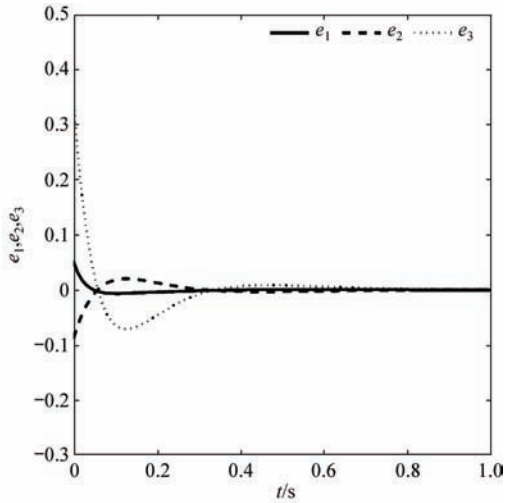

Fig. 6 Estimation error response of DOB.

Figs. 1-2 give the illustration of the reorientation maneuver in terms of inertial MRPs and angular velocities of both TVSMC and DOTVSMC, with the corresponding control torque commands in Fig. 3. It can be seen from Figs. 1-3 that the dynamic response processes are similar to each other for the two control algorithms. On the other hand, as shown in Fig. 4, there is a significant difference in the responses of the time-varying sliding functions. The time-varying functions of both TVSMC and DOTVSMC are both inside the predefined boundary layer thickness ($\xi_i = 0.001$). However, the magnitude of $\boldsymbol{S}(t)$ in TVSMC is about 4×10^{-4}, while 3×10^{-5} for DOTVSMC. As analyzed in Section 3.2, a precise performance would be achieved by DOTVSMC. According to the error MRP responses, the error MRP precision of TVSMC is about 2.6×10^{-4} while 1×10^{-8} for DOTVSMC, which indicates the improvement in the control accuracy of DOTVSMC.

Fig. 5 gives the comparison of the eigenaxis rotation performance between TVSMC and DOTVSMC. As the responses of angular velocity are similar as shown in Fig. 2, Fig. 5 provides a reliable evaluation of the eigenaxis rotation, which indicates that a precise eigenaxis rotation can be performed by DOTVSMC in the presence of inertia matrix uncertainty and external disturbance. The estimation error response is shown in Fig. 6, which verifies the fast convergence of the DOB.

Noticing that the control torque is actually provided by the on-off thrusters, which produce discontinuous and nonlinear control actions, we modulate the on-off thrusters by the pulse-width pulse-frequency (PWPF) modulator and give the proposed algorithms a further examination. The PWPF modulator is shown in Fig. 7, which is composed of a Schmitt trigger, a pre-filter and a feedback loop.

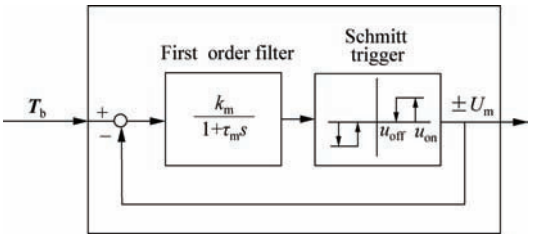

Fig. 7 Illustration of PWPF modulator.

In Fig. 7, $\boldsymbol{T}_b$ is the control torque command generated by the attitude control algorithms, k_m and τ_m are the filter gain and the time constant respectively, u_{on} and u_{off} are the on-value and off-value of Schmitt trigger, and U_m is the output of the Schmitt trigger. The output amplitude of the on-off thruster is supposed to 5 N·m, $k_m = 4.5$, $\tau_m = 0.15$, $u_{on} = 0.45$, $u_{off} = 0.15$. The principle of PWPF modulator and the selections of the related parameters can be referred to Ref. [21]. The simulation results are displayed in Figs. 8-11. Due to the space limitation, the time histories of the inertial MRP and angular velocity are omitted.

As shown in Fig. 8, excessive thruster actions exist during the steady state. It can be explained as follows: to guarantee the control accuracy, the deadband of the

PWPF modulator is selected as 0.1 N·m. While the lumped disturbance is actually larger than this minimum input, which will turn on the Schmitt trigger. If the deadband is selected larger, the thruster actions will be reduced while the control performance will be decreased correspondingly.

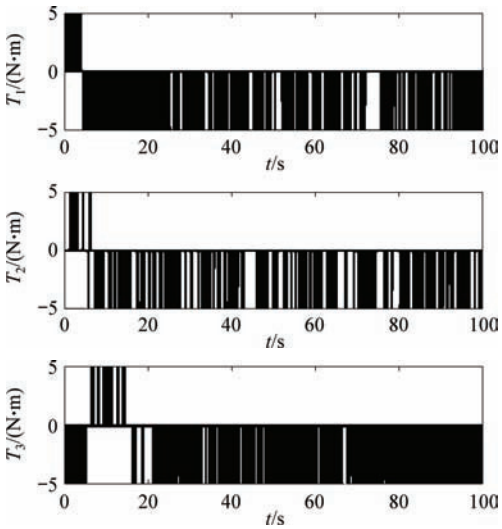

Fig. 8 On-off control torque of DOTVSMC.

With respect to the time-varying sliding functions responses, similar conclusions as the ideal condition ignoring the actuator dynamics can be drawn according to Fig. 9. The time-varying sliding functions are both inside the predefined boundary layer thickness all the time even the discontinuous on-off control torque is applied. The magnitude of $\boldsymbol{S}(t)$ can be kept within 1×10^{-4} by the DOTVSMC algorithm. The evaluation of the eigenaxis rotation performance is displayed in Fig. 10, which also indicates the improvement in the control accuracy of the DOTVSMC algorithm.

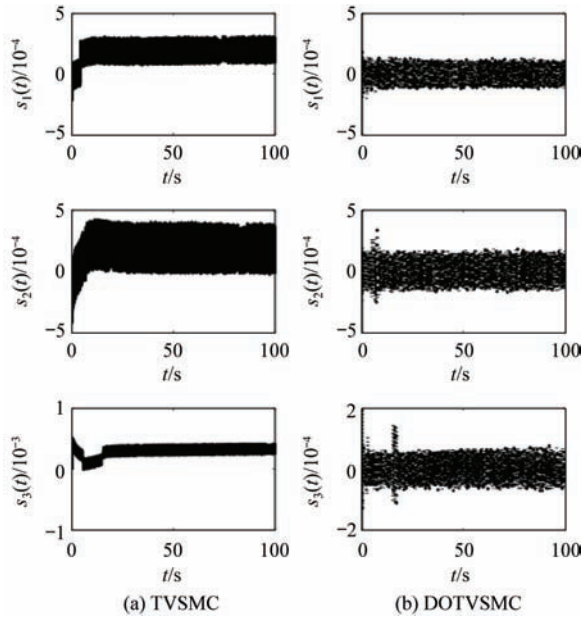

Fig. 9 Comparison of time-varying sliding functions with PWPF modulator.

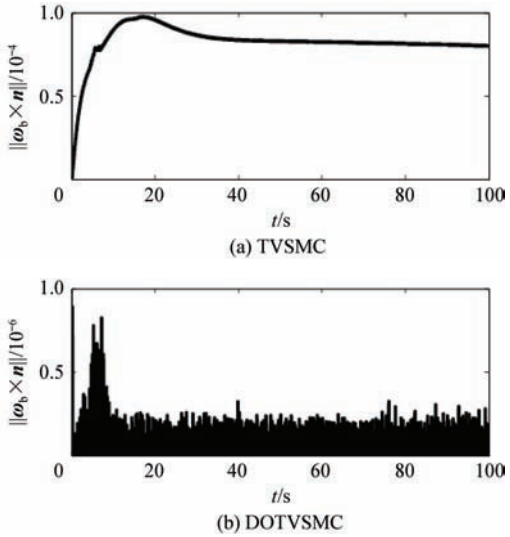

Fig. 10 Comparison of eigenaxis rotation performance with PWPF modulator.

Fig. 11 gives the estimation error responses of DOB. When PWPF modulator is used, the estimation error cannot converge to zero as depicted in Fig. 11. Even though the DOB cannot supply the controller with the correct estimation of the lumped disturbance, it does provide enough information for the controller.

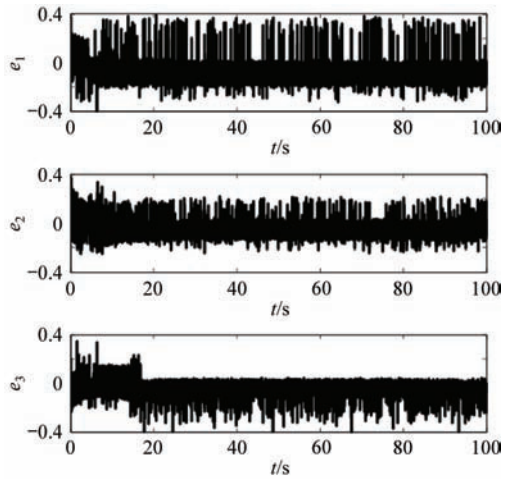

Fig. 11 Estimation error response of DOB with PWPF modulator.

5. Conclusions

In this paper, we have addressed the robust control problem of eigenaxis rotation for an uncertain rigid spacecraft via TVSMC technique. The proposed control strategy can guarantee the eigenaxis rotation performance in the presence of external disturbance and parametric uncertainty. The major contributions of this paper lie in three aspects. First, we extend the current results from the rest-to-rest maneuver to the reorientation maneuver and the necessary condition for the eigenaxis rotation is provided. Second, the global chattering problem, which is inherent in TVSMC, is solved by the boundary layer method and the disturbance ob-

server technique. The DOTVSMC algorithm is presented as a solution of the robust and precise eigenaxis rotation control. Finally, the proposed algorithms are tested with the on-off thrusters as the actuator, which have been proved to be feasible in engineering application.

References

[1] Milenkovic Z, Martin M. An implementation of an inertially-fixed eigenaxis attitude maneuver intercept algorithm. AIAA-2008-7298, 2008.

[2] D'Amario L A, Stubbs G S. A new single axis autopilot for rapid spacecraft attitude maneuvers. Journal of Guidance, Control, and Dynamics 1979; 2(4): 339-346.

[3] Wie B, Weiss H, Arapostathis A. Quaternion feedback regulator for spacecraft eigenaxis rotations. Journal of Guidance, Control, and Dynamics 1989; 12(3): 375-380.

[4] Wie B, Lu J B. Feedback control logic for spacecraft eigenaxis rotations under slew rate and control constraints. Journal of Guidance, Control, and Dynamics 1995; 18(6): 1372-1379.

[5] Seywald H, Lim K B, Anthony T C. Stability analysis for constrained principal axis slew maneuvers. Aerospace Sciences Meeting and Exhibit. 1997.

[6] Steyn W H. Near-minimum-time eigenaxis rotation maneuvers using reaction wheels. Journal of Guidance, Control, and Dynamics 1995; 18(5): 1184-1189.

[7] Chen X J, Steyn W H. Robust combined eigenaxis slew manoeuvre. AIAA-1999-4048, 1999.

[8] Lawton J R, Beard R W. Synchronized multiple spacecraft rotations. Automatica 2002; 38(8): 1359-1364.

[9] Ulrich S, Kron A, Lafontaine J D. Attitude guidance and control for synchronized maneuvers about a fixed rotation axis. AIAA-2008-7018, 2008.

[10] Cristi R, Burl J, Russo N. Adaptive quaternion feedback regulation for eigenaxis rotations. Journal of Guidance, Control, and Dynamics 1994; 17(6): 1287-1291.

[11] Lawton J R, Beard R W. Model independent eigenaxis maneuvers using quaternion feedback. IEEE Proceedings of American Control Conference. 2001; 2339-2344.

[12] Jan Y W, Chiou J C. Minimum-time spacecraft maneuver using sliding-mode control. Acta Astronautica 2004; 54(1): 69-75.

[13] Cong B L, Liu X D, Chen Z. Exponential time-varying sliding mode control for large angle attitude eigenaxis maneuver of rigid spacecraft. Chinese Journal of Aeronautics 2010; 23(4): 447-453.

[14] Tu S C. Attitude dynamics and control of satellite. Beijing: China Astronautic Publishing House, 2002. [in Chinese]

[15] Schaub H, Junkins J L. Analytical mechanics of space systems. 2nd ed. Virginia: AIAA, 2009.

[16] Etter J R. A solution of the time-optimal Euler rotation problem. AIAA-1989-3601, 1989.

[17] Bartoszewicz A. Time-varying sliding modes for second-order systems. IEE Proceedings of Control Theory and Applications 1996; 143(5): 455-462.

[18] Bhat S, Bernstein D. A topological obstruction to continuous global stabilization of rotational motion and the unwinding phenomenon. Systems & Control Letters 2000; 39(1): 63-70.

[19] Johnson C D. A new approach to adaptive control. In Leondes C T, editor. Control and Dynamic Systems. New York: Academic Press Inc., 1988: 1-69.

[20] Chen W H. Disturbance observer based control for nonlinear systems. IEEE/ASME Transactions on Mechatronics 2004; 9(4): 706-710.

[21] Song G B, Buck N V, Agrawal B N. Spacecraft vibration reduction using pulse-width pulse-frequency modulated input shaper. Journal of Guidance, Control, and Dynamics 1999; 22(3): 433-440.

Biographies:

CONG Binglong Born in 1984, he received his B.S. degree from Wuhan University in 2006 and M.S. degree from Beijing Institute of Technology (BIT) in 2009. He is now pursing the Ph.D. degree in BIT. His research interests include spacecraft attitude control, attitude coordination control for formation flying.
E-mail: cbl@bit.edu.cn

LIU Xiangdong Born in 1971, he received M.S. and Ph.D. degrees from Harbin Institute of Technology (HIT) in 1992 and 1995, respectively. From 1998 to 2000, he did his post doctor research in mechanical postdoctoral research center in HIT. He is currently a professor with school of automation in BIT. His research interests include high-precision servo control, spacecraft attitude control, Chaos theory.
E-mail: xdliu@bit.edu.cn

Appendix A: Proof of Lemma 1

Differentiating the Lyapunov function in Eq. (12) with respect to time, we can get

$$\dot{V} = \boldsymbol{S}^{\mathrm{T}}(t)(\boldsymbol{T}_{\mathrm{b}} + \boldsymbol{\Delta}_{\mathrm{du}} - \boldsymbol{\omega}_{\mathrm{b}}^{\times}\hat{\boldsymbol{J}}_{\mathrm{b}}\boldsymbol{\omega}_{\mathrm{b}}) + \lambda \boldsymbol{S}^{\mathrm{T}}(t)\frac{\hat{\boldsymbol{J}}_{\mathrm{b}}(4\boldsymbol{M}^{\mathrm{T}} - 2\boldsymbol{\sigma}_{\mathrm{e}}\boldsymbol{\sigma}_{\mathrm{e}}^{\mathrm{T}})\boldsymbol{\omega}_{\mathrm{b}}}{1+\|\boldsymbol{\sigma}_{\mathrm{e}}\|^2} - \lambda \boldsymbol{S}^{\mathrm{T}}(t)\hat{\boldsymbol{J}}_{\mathrm{b}}\left[\frac{\mathrm{d}}{\mathrm{d}t}\left(\frac{\boldsymbol{M}\boldsymbol{\zeta}}{m}\right) - \frac{\lambda \boldsymbol{M}\boldsymbol{\zeta}}{m}\right]\mathrm{e}^{-\lambda t} \quad \text{(A1)}$$

By substituting Eq. (13) into Eq. (A1), we can get

$$\dot{V} = \boldsymbol{S}^{\mathrm{T}}(t)(\boldsymbol{\Delta}_{\mathrm{du}} - \boldsymbol{\Gamma}\operatorname{sgn}\boldsymbol{S}(t)) \le -\sum_{i=1}^{3}(\gamma_i - d_{\max})\,|\,s_i(t)\,| \le 0 \quad \text{(A2)}$$

Clearly, for any $\boldsymbol{S}(t)\in\mathbf{R}^3$, $\dot{V}$ is non-positive and hence $V \le V(0)$. According to the fundamental idea of TVSMC technique, the initial value of the time-varying sliding function is zero, which results in $V(0) = 0$. Then we have $V \le 0$. On the other hand, it is obvious that $V \ge 0$ for any $\boldsymbol{S}(t)\in\mathbf{R}^3$ from Eq. (12). Therefore, it is easy to conclude that $V \equiv 0$, which implies that $\boldsymbol{S}(t) \equiv \boldsymbol{0}$ for $\forall t\in[0,\infty)$.